Sensors and Actuators B 155 (2011) 361–365

Contents lists available at ScienceDirect

Sensors and Actuators B: Chemical

journal homepage: www.elsevier.com/locate/snb

Short communication

Fast surface plasmon resonance imaging sensor using Radon transform

A. Karabchevsky*, S. Karabchevsky, I. Abdulhalim

Department of Electro Optic Engineering and The Ilse Katz Institute for Nanoscale Science and Technology, Ben Gurion University of the Negev, Beer Sheva 84105, Israel

ARTICLE INFO

Article history:
Received 20 September 2010
Received in revised form
29 November 2010
Accepted 3 December 2010
Available online 16 December 2010

Keywords:
Surface plasmon resonance
Imaging
Radon transform
Biosensing

ABSTRACT

Surface plasmon resonance (SPR) imaging technique is proposed in which a diverging laser beam at given frequency was used to illuminate the entire sensor surface in Kretschmann–Raether configuration. A pattern of dark intensity line on bright background is observed corresponding to the SPR dip at an angular range depending on the refractive index of the adjacent analyte and monitored by a two-dimensional CCD detector. A novel Radon transform based detection algorithm for the SPR line pattern is proposed, which is non sensitive to the laser speckle noise and improves the accuracy.

Over the last 15 years surface plasmon resonance (SPR) has become an undisputable leading technology for label-free detection and studies of biological binding to the sensor surface [1]. The detection limit of SPR technology is estimated as 1 pg/mm^2. Limit of detection (LoD) of commercially available SPR sensors is estimated as 10^{-6} to 10^{-5} refractive index units (RIU) for various sensor implementations with angular, spectral or intensity interrogations. Commercial SPR sensors such as BIAcore 3000 offer the baseline noise lower than 10^{-7} RIU [2]. Study of noise in SPR sensors and development of optimized algorithms for data processing of the SPR sensors have received much attention lately. One of the SPR data analysis approaches is minimal hunt method [3] by fitting a similar function to a portion of the data surrounding the most attenuated wavelength (wavelength interrogation) or angle (angular interrogation) using analytical derivative to find its minimum. Since the reflectivity response (versus angle or wavelength) is highly nonlinear, it is difficult to fit to it analytically. An alternative to the minimum hunt technique is a straightforward application of a center of mass calculation [3]. The center of mass of the resulting resonant dip is directly dependent on the depth and width of the resonance because it is asymmetric curve and therefore it is not a highly repeatable metric. Another data analysis method is the locally weighted parametric regression (LWPR) [4] which uses regression technique to calibrate location-shifting signals such as those produced by SPR. The LWPR method has been developed to the calibration of wavelength-modulated SPR sensors. This calibration method combines LWPR and nonlinear principal components regression (NPCR). It was shown that LWPR provides a calibration model that is more robust to random errors than traditional minima hunt calibration methods applied to SPR sensors [4]. Linearization of data processing algorithms and an optimal linear data analysis method were proposed as a means of optimizing algorithm parameters [5]. In our research we propose Radon transform based algorithm to analyze the SPR noisy data which is much simpler and straightforward than the previously proposed methods. In addition due to Radon transform integration behavior it is totally insensitive to any type of random granular noise.

There are several other methods to improve the SPR sensors resolution such as the long-range SPR configuration, wherein the evanescent field of the SPR on the metal surface is extended by inserting a dielectric buffer layer (of refractive index lower than that of water, for example Teflon) between the substrate and the metal [6]. This configuration significantly improves the detection limit as the attained refractive-index detection limit is 3×10^{-7} for amplitude SPR and 5.5×10^{-8} for phase SPR, which is the highest, reported so far [1,6,7]. Sensitivity enhancement is still under extensive research [8]. Such small detection limits combined with miniature multi-sensing devices will have applications in the future for integration into small spaces such as bottles of milk or in space missions where weight and volume have to be very small. A significant trend in medicine is the introduction of point of care devices for rapid, bedside diagnosis. These devices enable rapid diagnosis by first responders or medical staff for time-critical diagnoses, such as for indicating whether patients are presenting with cardiac symptoms. An initial clinical need is a sensor that can monitor and detect the presence of infections in intensive care patients. Currently, many intensive care patients develop infections that are not detected quickly, often leading to sepsis or shock and resulting in a

* Corresponding author.
E-mail address: rudenko@bgu.ac.il (A. Karabchevsky).

0925-4005/$ – see front matter © 2010 Elsevier B.V. All rights reserved.
doi:10.1016/j.snb.2010.12.012

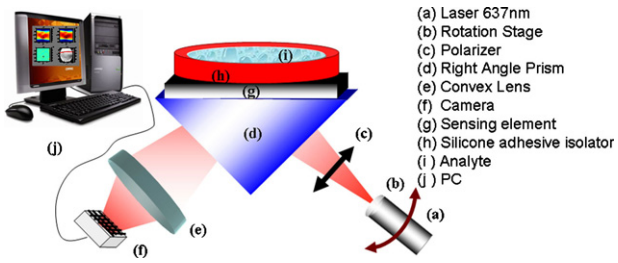

Fig. 1. Optical set-up.

large mortality rate. There is a significant need for sensors that can continuously and rapidly track the concentration of specific protein markers in a patient's bloodstream that are indicative of an infection, for instance.

The most popular SPR sensing scheme uses the prism coupling in the Kretschmann–Raether (KR) arrangement [9]. In KR configuration, reflectivity is measured as a function of angle of incidence, called angular modulation (AM), or wavelength, called wavelength modulation (WM). In the AM a single wavelength is used and a collimated laser beam incident on the metal film through the prism scanned over the incidence angles. The SPR dip is observed in the reflectivity versus incidence angle spectrum. Although the AM uses a single frequency and a collimated beam, the required scanning is problematic in particular when high accuracy and fast speed are required. Using an imaging scheme, the possibility of detecting arrays or imaging surfaces with very low contrast was demonstrated [10–12]. In these publications however the incident beam is usually a parallel beam focused (or non focused) on the metal–analyte surface and the surface is imaged with a lens and camera. In a less known configuration a converging [13] or diverging beam [14] is used which contains a wide range of angles and the divergent output beam falls on a detector array so that the SPR signal of reflectivity versus angle is obtained in a parallel manner without the need for scanning. In this article we demonstrate a fast and accurate SPR sensor that overcomes the problems associated with mechanical scanning using a single frequency diverging beam combined with a camera and special processing algorithm that helps in reducing the effects of speckle noise. Diverging incidence laser beam contains a range of spatial frequencies (angles) that will excite SPs, causing the appearance of a dark line perpendicular to the surface wave propagation. Such sensor enables immediate detection of analytes.

The excitation of plasmons by transverse magnetic-polarized coherent light requires a prism which matches between the k vector of the incidence light and the k vector of the plasma [9]:

$$\sqrt{\varepsilon_p}\sin\theta_p = Re\left\{\sqrt{\frac{\varepsilon_m\varepsilon_d}{\varepsilon_m+\varepsilon_d}}\right\} \quad (1)$$

where ε_p is dielectric constant of the prism, θ_p defined as: $k_x = \sqrt{\varepsilon_p}(\omega/c)\sin\theta_p$ while c is the light velocity in free space and ω is radiant frequency. ε_m and ε_d are the complex dielectric constants of the metal and dielectric (analyte), respectively. A surface wave is excited due to attenuated total internal reflection of the light at the interface between the metal and dielectric [9]. According to Eq. (1) the SP can be excited at a specific angle depending on the light wavelength through the materials dispersion relation. Hence in order to be able to work in the diverging beam mode the beam divergence should be larger than the full width at half maximum (FWHM), roughly at least 3 times the FWHM. For ideal silver film on SF11 glass in the case of ethanol in water analyte, FWHM varies between 0.45° (for pure water) till 1.55° (for pure ethanol).

To demonstrate the concept presented in previous paragraph silver layers (70 nm thickness) were deposited on SF11 and BK7

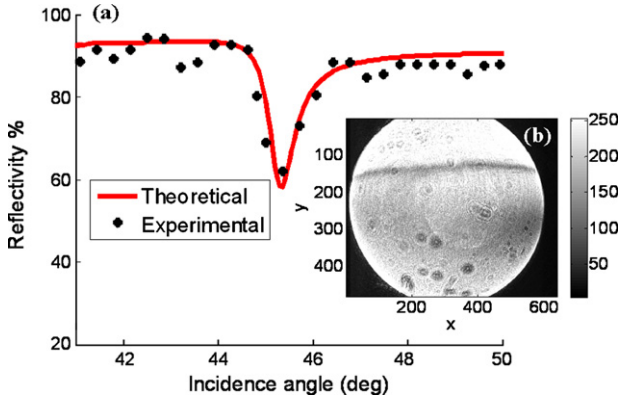

Fig. 2. SPR reflection patterns in air: (a) reflection as a function of the internal incidence angle, experimental (black dots) using KR arrangement and theoretical (red line), (b) typical image (taken using the set-up in Fig. 1) while SP is excited. (For interpretation of the references to color in this figure caption, the reader is referred to the web version of the article.)

glass slides. A thin layer of SiO_2 (~21 nm thickness) was deposited on top of the silver film for protection from oxidation. For the sensing elements (Ag deposed on glass substrates samples with or without anti-oxidation layer) on BK7 the FWHM is 0.3° in air with the SiO_2 layer. *Note*: However, the parameters of the sensing element are not ideal, it is good enough to demonstrate the concept. The samples were characterized first using the standard KR arrangement while the incident laser beam at 637 nm was collimated. To perform the experiment with a diverging beam, the setup shown in Fig. 1 was used where the 637 nm laser diode is diverging such that the beam incident on the prism cathetus has diameter smaller than the cathetus width. The convex lens in front of the camera was added to collect the beam so that it fits the active area of the camera sensor. The sample is held on the base of the prism horizontally for convenience while adding liquids as shown in Fig. 1. Output images acquired by the camera were processed using Matlab. The proposed setup is very useful for sensing applications in liquids since the prism and the sensing element are oriented horizontally, which enables dripping of the analyte on top of the sensing element into adhesive silicone isolator (Sigma product).

Fig. 2(a) shows reflection as a function of the incidence angle from one of the investigated samples which were characterized using standard KR arrangement with appropriate theoretical fit when the analyte is air. One of the typical images acquired with the camera is shown in Fig. 2(b). Due to expanding light source (see Fig. 2(a)), a dark line is obtained on the bright background. This dark line will be shifted parallel to the previous one when different analytes are applied to the metal surface as it will be explained in Fig. 4. As it can be seen from Fig. 2(b) the acquired SPR image is highly affected by a speckle noise. A speckle noise is a random intensity pattern produced by the interference of a set of random wave fronts, which produces a resultant wave whose amplitude, and therefore intensity, varies randomly. In order to locate the SPR dark line in highly speckled SPR image we propose a Radon transform (RT) [15] (named after the Austrian mathematician Johann Radon (1917)) based algorithm which is not sensitive to the speckle noise. The RT in polar coordinates is defined as follows [15]:

$$(\Re f) \equiv g(\rho,\theta) = \int_{-\infty}^{\infty}\int_{-\infty}^{\infty} f(x,y)\delta(x\cos\theta + y\sin\theta - \rho)dxdy$$

$$= \int_{-\infty}^{\infty} f(\rho\cos\theta - l\sin\theta,\quad \rho\sin\theta - l\cos\theta)dl \quad (2)$$

where $f(x, y)$ is a two-dimensional function which represents the image, $\rho = \sqrt{x^2+y^2}$ and $\theta \in [-90°, 90°]$ are the radial the

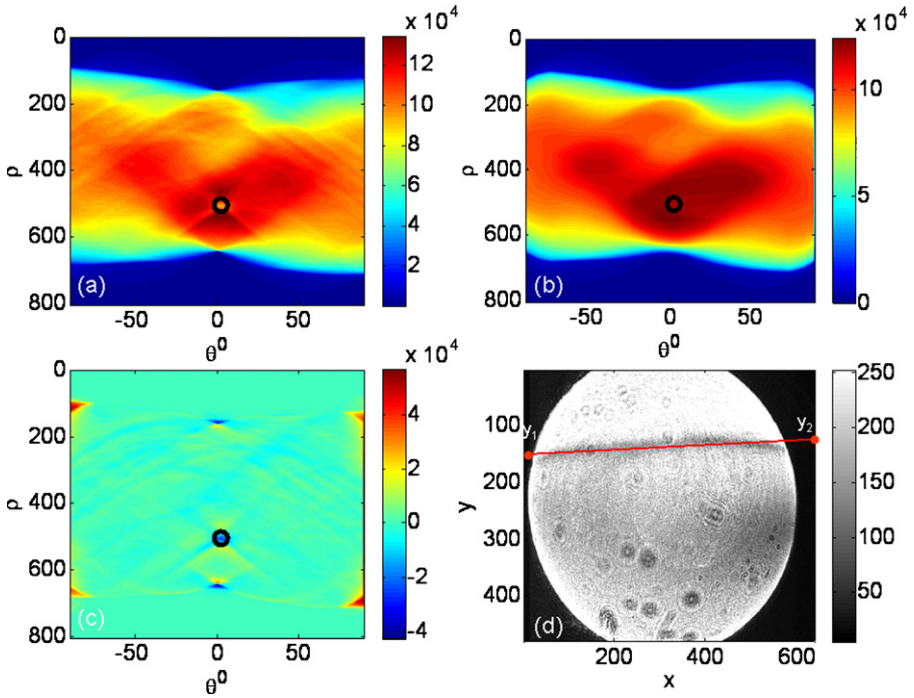

Fig. 3. (a) RT of original image: $g(\rho, \theta)$, (b) background: $MF^{31\times31}\{g\}(\rho, \theta)$, (c) background suppression: $g(\rho, \theta)_{BS}$. *Note*: The circle marks minima which relates to the wanted line in the image domain. (d) SPR image: $f(x, y)$ which was shown in Fig. 2b with recognized SPR location designated by red line. (For interpretation of the references to color in this figure caption, the reader is referred to the web version of the article.)

polar coordinates, respectively. The Dirac δ-function converts the two-dimensional integral to a line integral along the line $x\cos\theta + y\sin\theta = \rho$; (x, y) are the pixel coordinates in the image: $x \in [0, m]$ and $y \in [0, n]$ with $m \times n$ being the dimensions of the camera sensor in pixels. To translate pixels to degrees, each coordinate should be multiplied by the angular pixel size. The function $f(x, y)$, (obtained image using the set-up in Fig. 1) represents unknown reflection from sensing element, and then $g_{\min}(\rho, \theta)$ (in Radon space) represents the parameters of the SPR line at given analyte. Due to the integration along the line, RT is sensitive to line patterns, a property that is highly useful in our case. In addition, the integration along the line partially averages the speckle noise.

Fig. 3(a) shows the RT domain for the image in Fig. 2(b). Each point (ρ, θ) in the RT domain represents a single line in the xy image domain. The location of the SPR dark line is represented by the local intensity minimum $g_{\min}(\rho, \theta)$ in the RT domain designated by a black circle in Fig. 3(a). However, additional minimal points may occur due to: (a) noisy image, (b) different shapes and (c) non uniform illumination. This will lead to inaccuracy in the recognition of the desired local minimum. Additional unwanted minimal areas

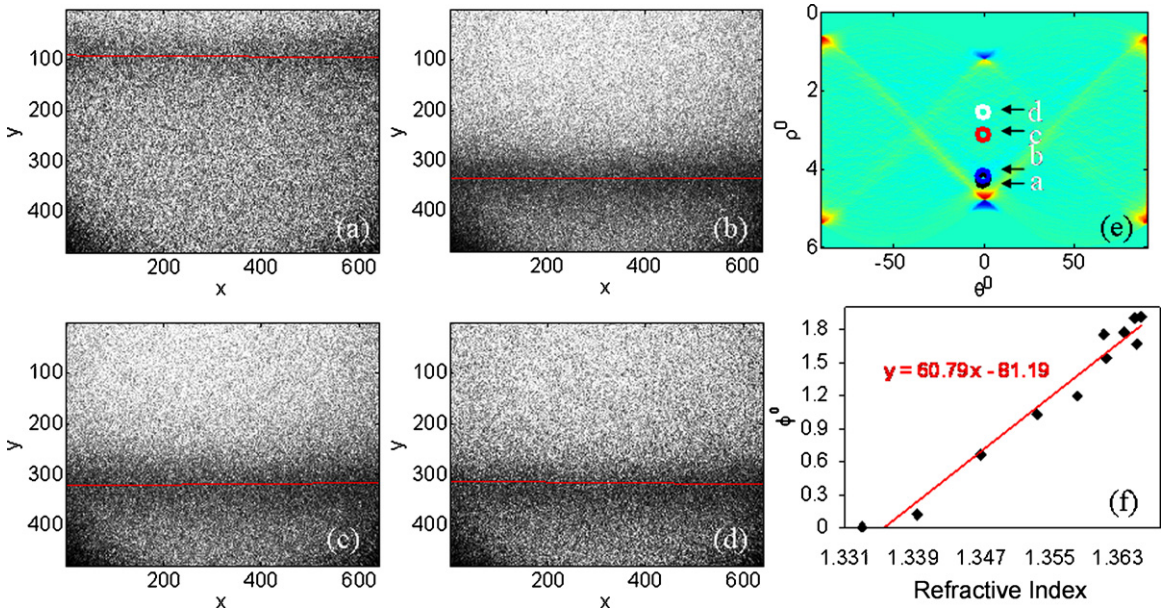

Fig. 4. Some of the experimental results of the SPR imaging: (a)–(d) ethanol diluted in DI solutions: (a) 100% DI, (b) 10% ethanol in 90% DI, (c) 40% ethanol in 60% DI and (d) 100% ethanol; (e) location of the SPR lines in Radon space; (f) locations of resonances achieved experimentally as a function of the RI of ethanol concentrations diluted in water [20] and estimated regression line.

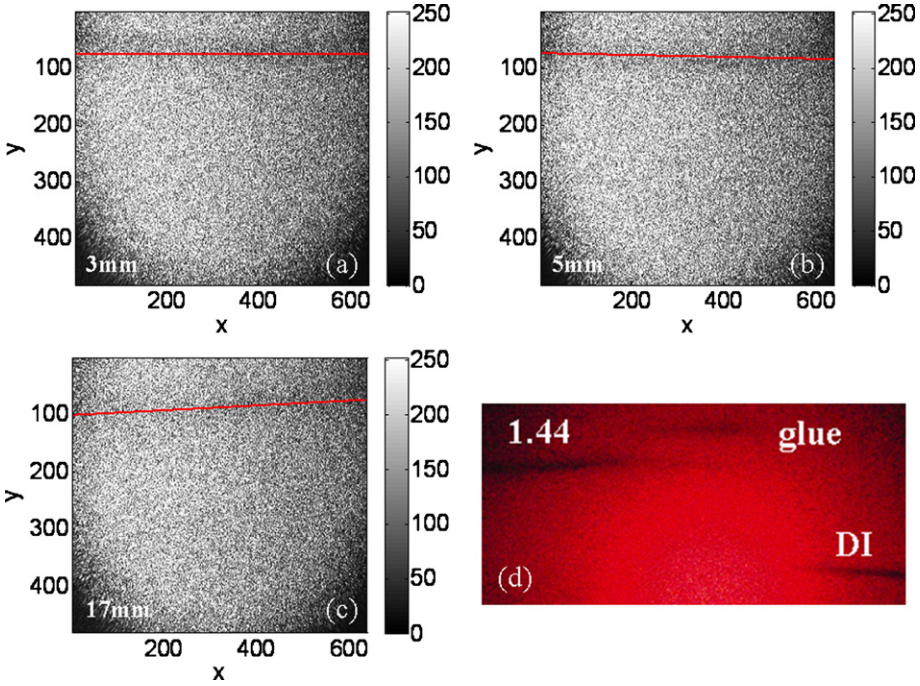

Fig. 5. SPR imaging output: (a) SPR of the sensing element in air while it is moved on the prism with steps shown in each image relative to the initial position; (b) triple channel SPR: oil with RI 1.44, glue and DI (RI of 1.3325).

(obtained due to noisy image) will not be well defined and can be treated as a background. A background suppression technique needs to be carried out in order to suppress that unwanted minima, this is a common technique in sonar image processing for target detection [16]. The background suppression involves subtracting an estimated background using a 31×31 median filter operator ($MF^{31\times31}$) (Fig. 3(b)) from the Radon transform image (Fig. 3(a)). A result after background suppression (BS): $g(\rho, \theta)_{\mathrm{BS}}$ is shown in Fig. 3(c), and can be described by the following formula:

$$g(\rho, \theta)_{\mathrm{BS}} = g(\rho, \theta) - MF^{31\times31}\{g\}(\rho, \theta) \tag{3}$$

Fig. 3(d) shows the line position (red line) using the proposed algorithm. The start and the end points (symbolized by y_1 and y_2, respectively) show location of the line in pixels. Some of the experimental results using different ethanol concentrations in DI solutions are presented in Fig. 4(a1–a4). In this figure the samples that were used are 70 nm Ag deposited on SF11 glass and immersed in 1 mM long chain thiol 11-MUA (Sigma product) for 24 h to prevent silver from oxidation [17] and for further use to immobilize antibodies. The same experimental set-up shown in Fig. 1 was used when the laser beam passed through an optical fiber for homogenization of the beam. Extracted location of the SPR line (in degrees) pattern using the proposed algorithm is shown in Fig. 4(a1–a4) and altogether in Fig. 4(b). Fig. 4(c) shows the minimal intensity values detected in Radon space while each circle color designates one analyte solution. Fig. 4(d) shows extracted SPR line locations as a function of the analyte RIs.

The sensitivity of the sensor, which is evaluated from the regression line estimation, is $\Delta\phi^{\circ}/\Delta n = 60.79^{\circ}$/RIU. Theoretical calculations provided 61.74°/RIU sensitivity for given parameters of the sensor (RIs of the analyte, SF11 prism and the metal for incident wavelength of 637 nm) as was achieved experimentally with the proposed SPR imaging sensor. To be able to analyze the sensitivity of the proposed sensor, it is necessary to know the angular position of the SPR line and the angular pixel size. The angular shift in degrees $\Delta\phi^{\circ}$ is defined as follows:

$$\Delta\phi^{\circ} = \frac{\Delta p \delta\phi}{n} \tag{4}$$

where Δp is the shift in pixels of the dark line with respect to the reference line (in our case de-ionized water – DI). $\delta\phi = D_{lens}{\cdot}NA/(D_{spot}{\cdot}n)$ is the angular pixel size in degrees: D_{lens} is the diameter of the lens (see Fig. 1(e)), D_{spot} is the diameter of the spot incident on the lens normal to the SPR line, NA is the numerical aperture of the fiber (here 0.55) and n is the dimension of the camera normal to the SPR line (the camera used by us has $m \times n = 659 \times 494$ pixels). Hence the pixel size in our case is $\delta\phi = 0.0078^{\circ}$. The limit of detection (LoD) or the resolution of the sensor is determined by the ratio between the noise level and the sensitivity: $\mathrm{LoD} = \langle \delta\phi \rangle / S_{\phi}$ where $S_{\phi} = \Delta\phi/\Delta(\mathrm{RI})$ is the angular sensitivity. Since the line is composed of m data points (pixels), and the minimum detectable angular shift is determined by the noise level which is a single pixel that corresponds to $\delta\phi = 0.0078^{\circ}$, the LoD is given by:

$$\mathrm{LoD} = \frac{\delta\phi}{\sqrt{m}} \left(\frac{\Delta\phi}{\Delta(\mathrm{RI})} \right)^{-1} \tag{5}$$

Experimentally the estimated LoD is 5×10^{-6} RIU. Note that the fact that we have a line composed of m pixels, improves our accuracy by a factor of $\sqrt{m}$. This is another advantage of the present technique over the standard angular scanning SPR technique or the SPR imaging technique with collimated beam [18]. To achieve the ideal LoD one can optimize the system further such as using more divergence of the beam and using a camera with larger number of pixels to decrease the pixel size. One can also use inverse scattering approaches such as theoretical calculation of reflectivity versus incidence angle and fit it with experimental results to achieve subpixel resolution. Fig. 5 shows another possible application of the proposed SPR imaging sensor. Fig. 5(a)–(d) shows results of the homogeneity of deposed silver layer on glass by moving the sensing element from its original position. Multichannel sensing is shown in Fig. 5d where three different RI shifts the SPR line differently: 1.44 oil, glue of the silicone adhesive isolator and DI.

To conclude, the fast SPR imaging sensor is demonstrated using diverging laser beam and a camera in KR arrangement combined with Radon transform. A pattern of dark intensity line (perpendicular to the edge of the prism cathetus) on bright area was imaged at angular range depending on the dielectric constant of the analyte. An efficient detection algorithm based on Radon transform was introduced for SPR location extraction with less sensitivity to laser speckle and nonuniformity of the illumination. This enabled characterization of the analyte RI changes in terms of dark intensity line location with sensitivity of 60.79°/RIU and detection limit of 5×10^{-6} RIU in a bench type setup. We believe that it is possible to improve the sensor resolution by 1–2 orders of magnitude as follows: (i) reducing the pixel size for example using larger divergence of the beam or using a camera with smaller pixels, (ii) increasing the number of pixels perpendicular to the SPR line, (iii) increasing the angular sensitivity for example by adding a dielectric top nanolayer with high index [8] or reducing the prism index [19], (iv) using the possibility of a reference SPR line using a channel with liquid of the same thermooptic coefficient as the analyte being sensed. This latter option was in fact shown in Fig. 5d where SPR line of different materials is presented.

Such sensor may find variety of applications: (1) detection of degree of homogeneity of the surface (Fig. 5a) and the ambient – chemical compound (for non homogeneous compounds the SPR line will appear as curve); (2) evaporation time of materials – SPR line will change its location with time; (3) microbial and enzyme detection for environmental monitoring; (4) monitoring of immunoreactions; (5) olfactory device (odor sensing system) which can replace or complement human sensory tests in fields of food, drink, cosmetics and environmental control using odorant binding proteins (OBPs), etc.

Acknowledgements

This work is supported by the Ministry of Science under Tashtiot program. We acknowledge Mr. Lev Tsapovsly and Prof. Robert Marks from biotechnology engineering department for help in preparing 11-MUA based solution for preventing silver samples from oxidation.

References

[1] I. Abdulhalim, M. Zourob, A. Lakhtakia, Surface plasmon resonance for biosensing: a mini-review, Electromagnetics 28 (2008) 214–242.
[2] J. Homola, S.S. Yee, G. Gauglitz, Surface plasmon resonance sensors: review, Sensors and Actuators B: Chemical 54 (1999) 3–15.
[3] K.S. Johnston, K.S. Booksh, T.M. Chinowsky, S.S. Yee, Performance comparison between high and low resolution spectrophotometers used in a white light surface plasmon resonance sensor, Sensors and Actuators B: Chemical 54 (1999) 80–88.
[4] K.S. Johnston, S.S. Yee, K.S. Booksh, Calibration of surface plasmon resonance refractometers using locally weighted parametric regression, Analytical Chemistry 69 (1997) 1844–1851.
[5] Chinowsky, Optimal linear data analysis for surface plasmon resonance biosensors, Sensors and Actuators A: Physical 54 (1999) 89.
[6] R. Slavík, J. Homola, Ultrahigh resolution long range surface plasmon-based sensor, Sensors and Actuators B: Chemical 123 (2007) 10–12.
[7] A.V. Kabashin, S. Patskovsky, A.N. Grigorenko, Phase and amplitude sensitivities in surface plasmon resonance bio and chemical sensing, Optics Express 17 (2009) 21191–21204.
[8] A. Lahav, M. Auslender, I. Abdulhalim, Sensitivity enhancement of guided-wave surface-plasmon resonance sensors, Optics Letters (Ol) 33 (2008) 2539.
[9] H. Raether, Surface Plasmons on Smooth and Rough Surfaces and on Gratings (Springer Tracts in Modern Physics), vol. 111, Springer-Verlag, Berlin, New York, 1988.
[10] B. Rothenhausler, W. Knoll, Surface-plasmon microscopy, Nature 332 (1988) 615–617.
[11] G. Steiner, Surface plasmon resonance imaging, Analytical and Bioanalytical Chemistry 379 (2004) 328–331.
[12] K.D. Kihm, Surface plasmon resonance reflectance imaging technique for near-field (~100 nm) fluidic characterization, Experiments in Fluids 48 (2010) 547–564.
[13] M. Zourob, S. Elwary, A. Turner, A.D. Taylor, J. Ladd, J. Homola, S. Jiang, Surface plasmon resonance (SPR) sensors for the detection of bacterial pathogens, in: Principles of Bacterial Detection: Biosensors, Recognition Receptors and Microsystems, Springer, New York, 2008, pp. 83–108.
[14] R.B.M. Schasfoort, A.J. Tudos, Handbook of Surface Plasmon Resonance, Royal Society of Chemistry, Cambridge, 2008.
[15] S. Helgason, The Radon Transform, 2nd ed., Series in Mathematics (Boston, Mass.), vol. 5, 1999, Boston.
[16] M.J. Chantler, J.P. Stoner, Automatic Interpretation of Sonar Image Sequences Using Temporal Feature Measures: Special Issue on Image Processing for Oceanic Applications, vol. 22, Institute of Electrical and Electronics Engineers, New York, NY, 1997, ETATS-UNIS.
[17] A. Abdelghani, J.M. Chovelon, J.M. Krafft, N. Jaffrezic-Renault, A. Trouillet, C. Veillas, C. Ronot-Trioli, H. Gagnaire, Study of self-assembled monolayers of n-alkanethiol on a surface plasmon resonance fibre optic sensor, Thin Solid Films 284–285 (1996) 157–161.
[18] J.D. Swalen, J.G. Gordon, M.R. Philopott, A. Brillante, I. Pockrand, R. Santo, Plasmon surface polariton dispersion by direct optical observation, American Journal of Physics 48 (1980).
[19] A. Shalabney, I. Abdulhalim, Electromagnetic fields distribution in multilayer thin film structures and the origin of sensitivity enhancement in surface plasmon resonance sensors, Sensors and Actuators A: Physical 159 (2010) 24–32.
[20] R.C. Weast, M.J. Astle, Handbook of Chemistry and Physics, vol. 57, CRC Press, Boca Raton, FL, 1979.

Biographies

Alina Karabchevsky was born in March 9, 1980 in Vinnica, Ukrain. She received her bachelor and master of sciences in biomedical engineering from the Ben-Gurion University of the Negev, Beer-Sheva, Israel in 2005 and 2008, respectively. During her master degree she specialized on biomedical signal processing. Currently, she is a Ph.D. student in electro-optics engineering at Ben Gurion University. Recently she organized an SPIE student chapter at Ben-Gurion University. Her research interests are plasmonic nano-structures and optical biosensing devices both combines her biomedical engineering background with optics and physics.

Serge Karabchevsky was born in January 11, 1979 in Sant-Petersburg, Russia. He received his BSc in Electrical and Computer engineering from the Ben-Gurion University of the Negev, Beer-Sheva, Israel in 2005. He spent several years working in industry such as BATM Telecom and GIDEL. Currently he is studying for MSc in Electro-Optics Engineering at Ben Gurion University, Beer-Sheva, Israel. His research interests are FPGA Algorithms Architecture, Image Processing and Autonomous Robotics.

Prof. Ibrahim Abdulhalim was born in Kafr Manda, Israel in November 22, 1957. He studied Physics at the Technion, Haifa, where he received his BSc, MSc and DSc in 1982, 1985 and 1988, respectively. He spent several years working in applied optics in academia and industry such as in the University of Colorado at Boulder, in the ORC at Southampton University, in the University of Western Scotland, in KLA-Tencor Corporation, in Nova Measuring Instruments and in GWS-Photonics. In October 2005 he joined the Ben Gurion University, department of electro-optic engineering. His current research activities involve nanophotonic structures for biosensing, improved biomedical optical imaging techniques such as spectropolarimetric imaging and full field optical coherence tomography. Prof. Abdulhalim has published over 90 journal articles, 50 conference proceedings papers, and 10 patents. He became a fellow of the Institute of Physics, UK in 2004 and recently he became a fellows of SPIE. He is an associate editor of the SPIE Journal of NanoPhotonics for the fourth year now.